Multiple biochemical similarities between infectious and non-infectious aggregates of a prion protein carrying an octapeptide insertion

Emiliano Biasini,* Andrea Z. Medrano,* Stefano Thellung,*,[1] Roberto Chiesa† and David A. Harris*

*Department of Cell Biology and Physiology, Washington University School of Medicine, St Louis, Missouri, USA

†Dulbecco Telethon Institute and Department of Neuroscience, Istituto di Ricerche Farmacologiche "Mario Negri", Milan, Italy

Abstract

A nine-octapeptide insertion in the prion protein (PrP) gene is associated with an inherited form of human prion disease. Transgenic (Tg) mice that express the mouse homolog of this mutation (designated PG14) spontaneously accumulate in their brains an insoluble and weakly protease-resistant form of the mutant protein. This form (designated PG14^{Spon}) is highly neurotoxic, but is not infectious in animal bioassays. In contrast, when Tg(PG14) mice are inoculated with the Rocky Mountain Laboratory (RML) strain of prions, they accumulate a different form of PG14 PrP (designated PG14^{RML}) that is highly protease resistant and infectious in animal transmission experiments. We have been interested in characterizing the molecular properties of PG14^{Spon} and PG14^{RML}, with a view to identifying features that determine two, apparently distinct properties of PrP aggregates: their infectivity and their pathogenicity. In this paper, we have subjected PG14^{Spon} and PG14^{RML} to a panel of assays commonly used to distinguish infectious PrP (PrP^{Sc}) from cellular PrP (PrP^{C}), including immobilized metal affinity chromatography, precipitation with sodium phosphotungstate, and immunoprecipitation with PrP^{C}- and PrP^{Sc}-specific antibodies. Surprisingly, we found that aggregates of PG14^{Spon} and PG14^{RML} behave identically to each other, and to authentic PrP^{Sc}, in each of these biochemical assays. PG14^{Spon} however, in contrast to PG14^{RML} and PrP^{Sc}, was unable to seed the misfolding of PrP^{C} in an in vitro protein misfolding cyclic amplification reaction. Collectively, these results suggest that infectious and non-infectious aggregates of PrP share common structural features accounting for their toxicity, and that self-propagation of PrP involves more subtle molecular differences.

Keywords: neurodegeneration, prion, protein aggregates, prion protein, scrapie isoform of prion protein, transgenic mice.

J. Neurochem. (2008) **104**, 1293–1308.

Prion diseases are fatal neurodegenerative disorders of humans and animals characterized by dementia, motor dysfunction, and cerebral amyloidosis. A great deal of evidence indicates that the key event underlying all forms of prion diseases is the conformational conversion of the cellular prion protein (PrP^{C}) into an infectious isoform (scrapie isoform of PrP, PrP^{Sc}) that has a high content of β-sheet (Prusiner 1998; Weissmann 2004). PrP^{Sc} accumulates

in the CNS of affected individuals in an aggregated and protease-resistant form that is believed to propagate itself by impressing its conformation onto PrP^C substrate molecules. Prion diseases can be infectious, sporadic, or genetic in origin. About 10% of the cases of Creutzfeldt-Jakob disease and all cases of Gerstmann-Sträussler syndrome and fatal familial insomnia are inherited in an autosomal dominant fashion, and are linked to insertional and point mutations in the PrP gene on chromosome 20 (Kong *et al.* 2004). The insertional mutations consist of 1–9 additional copies of a peptide repeat (P(H/Q)GGG(-/G)WGQ) which is normally present in five copies. These mutations produce a phenotype which displays features of both Creutzfeldt-Jakob disease and Gerstmann-Sträussler syndrome. Disease-associated mutations in PrP are presumed to favor spontaneous conversion of PrP^C into PrP^{Sc} without the necessity for contact with exogenous infectious agent.

Although the basic mechanism of prion propagation has now been established, much less is known about how prions kill neurons and cause neuropathology (Chiesa and Harris 2001; Westergard *et al.* 2007). In particular, there is considerable uncertainty regarding the molecular identity of the PrP species that are directly responsible for prion-induced neurodegeneration. Although it has commonly been assumed that PrP^{Sc} is pathogenic, several pieces of evidence call this assumption into question. For example, some inherited cases of prion disease are not transmissible to laboratory animals, and are not associated with accumulation of conventional forms of protease-resistant PrP^{Sc} (Brown *et al.* 1994; Tateishi and Kitamoto 1995; Nazor *et al.* 2005; Piccardo *et al.* 2007). These and other data argue that alternative forms of PrP, distinct from both PrP^C and PrP^{Sc}, may be the primary neurotoxic species in some prion diseases. We have referred to such pathogenic molecules as PrP^{toxic} to distinguish them from infectious PrP^{Sc} (Chiesa and Harris 2001). It remains uncertain, however, what structural features distinguish PrP^{toxic} and PrP^{Sc}.

Clues to the molecular distinction between neurotoxic and infectious forms of PrP have emerged from studies of Tg(PG14) mice (Chiesa *et al.* 1998, 2000). These mice express the mouse PrP homolog of a nine-octapeptide repeat insertion that is linked to an inherited prion dementia in humans (Owen *et al.* 1992; Duchen *et al.* 1993; Krasemann *et al.* 1995). Tg(PG14) mice accumulate in their brains a form of mutant PrP that exhibits some of the biochemical properties of PrP^{Sc}, including protease resistance and propensity to aggregate. However, this form differs from PrP^{Sc} because it fails to transmit disease when inoculated intracerebrally into host mice (Chiesa *et al.* 2003). In addition, the mutant PrP exhibits considerably less protease resistance than conventional PrP^{Sc} (Chiesa *et al.* 1998). As PG14 PrP aggregates accumulate, Tg(PG14) mice develop a progressive, ultimately fatal, neurological disorder characterized by ataxia, Bax-dependent apoptosis of cerebellar granule cells, and Bax-independent loss of synaptic markers (Chiesa *et al.* 1998, 2005; Biasini *et al.* 2006). As PG14 PrP in Tg(PG14) mice is pathogenic but not infectious, it represents an example of PrP^{toxic} (Chiesa and Harris 2001).

When Tg(PG14) mice are inoculated with scrapie prions, they accumulate a form of PG14 PrP that is resistant to high concentrations of protease, and that is infectious upon serial passages (Chiesa *et al.* 2003). Thus, this scrapie-seeded form of PG14 PrP displays profoundly different biological and biochemical properties from the spontaneously generated, non-infectious form which is found in uninoculated Tg(PG14) mice. We have designated the spontaneous form as $PG14^{Spon}$ and the prion-seeded form as $PG14^{RML}$ (after the RML strain of scrapie used for inoculation) (Chiesa *et al.* 2003).

We have argued that understanding the molecular differences between $PG14^{Spon}$ and $PG14^{RML}$ will provide important insights into the nature of PrP^{toxic} and the features that endow PrP with infectivity. In a previous study, we undertook a preliminary characterization of these differences (Chiesa *et al.* 2003). We found that $PG14^{Spon}$ and $PG14^{RML}$ both displayed conformationally masked antibody epitopes in the central and octapeptide regions of the protein, similar to PrP^{Sc}. However, we observed that these two forms differed in their oligomeric states, with $PG14^{RML}$ aggregates being larger and more resistant to urea-induced dissociation. Based on these data, we suggested that differences in polymerization state (quaternary structure) could explain the disparity in protease resistance and infectivity between the two forms.

In this paper, we present a more exhaustive characterization of the properties of $PG14^{Spon}$ and $PG14^{RML}$, by applying a panel of biochemical assays commonly used to distinguish between PrP^C and PrP^{Sc}. Surprisingly, $PG14^{Spon}$ and $PG14^{RML}$ behave similarly in each of these assays, which include immobilized metal affinity chromatography (IMAC), sodium phosphotungstic acid (NaPTA) precipitation, and recognition by PrP^C- and PrP^{Sc}-specific antibodies. As part of this work, we have identified a soluble (non-aggregated) form of PG14 PrP that we refer to as $PG14^{Sol}$. $PG14^{Sol}$ displays the biochemical properties of PrP^C, and is likely to represent a precursor to aggregated forms of both $PG14^{Spon}$ and $PG14^{RML}$. Finally, we show that $PG14^{RML}$ but not $PG14^{Spon}$ is infectious, based on several *in vitro* tests, including the ability to seed conversion of wild-type (WT) PrP substrate in a protein misfolding cyclic amplification (PMCA) reaction (Saborio *et al.* 2001).

Cumulatively, our data demonstrate that, although $PG14^{Spon}$ and $PG14^{RML}$ are markedly different in terms of infectivity, they are strikingly similar in a number of biochemical properties. Thus, infectious and non-infectious aggregates of PrP are likely to share common structural features, some of which may underlie their neurotoxic activity. In contrast, infectivity may depend upon subtle

molecular differences between the aggregates, perhaps related to their pathway of oligomerization.

Materials and methods

Mice

Production of Tg mice expressing WT and PG14 mouse PrPs tagged with an epitope for the monoclonal antibody (mAb) 3F4 has been reported elsewhere (Chiesa *et al.* 1998). We used Tg(WT) mice of the E1 line that express four times the endogenous PrP level and remain healthy, and Tg(PG14) mice of the A3 line that express PG14 PrP at a level equivalent to endogenous PrP. These Tg mice were originally generated on a C57BL/6J X CBA/J hybrid background, and were subsequently bred with the Zürich I line of $Prn-p^{0/0}$ mice (C57BL/6J X 129 background) (Büeler *et al.* 1992). The resulting animals therefore express transgenically encoded but not endogenous mouse PrP. For some experiments, we bred Tg(PG14) mice to Tg(WT) mice to obtain doubly transgenic (Tg) animals expressing both PG14 and WT PrP.

For studies involving RML-infected mice, the RML isolate of scrapie was obtained from Byron Caughey and Richard Race (Rocky Mountain Laboratories, Hamilton, MT, USA) and was passaged repeatedly in CD1 (Swiss) mice. Ten percent (w/v) homogenates of mouse brain were prepared in phosphate-buffered saline (PBS) using sterile, disposable tissue grinders. After being cleared by centrifugation at 900 g for 5 min, the homogenates were diluted to a final concentration of 1% or 2.5% in PBS, and 25 μL was injected intracerebrally into the right parietal lobes of 4- to 6-week-old recipient mice using a 25-gauge needle.

Transgenic mice expressing WT PrP-EGFP (line A) (Barmada *et al.* 2004) were crossed with Tg(PG14) mice to produce bigenic progeny expressing both WT PrP-EGFP and PG14 PrP. Tg mice expressing PG14 PrP-EGFP will be described in a forthcoming publication (A. Medrano, S. J. Barmada, E. Biasini, and D. A. Harris; paper submitted).

Partial purification of PG14^{Spon} and PG14^{RML} by sequential centrifugation

Fractionation of brain homogenates was performed as previously described (Silveira *et al.* 2005). One mouse brain was cut in small pieces, washed with 1X PBS, homogenized with 3 mL of 10% sarcosine in 1X TEND (10 mmol/L Tris–HCl pH 8, 1 mmol/L EDTA, 130 mmol/L NaCl, and 1 mmol/L dithiothreitol) plus Complete® protease inhibitors (Roche, Indianapolis, IN, USA), then incubated on ice for 1 h and centrifuged at 22 000 g for 30 min at 4°C. The supernatant was incubated on ice, while the pellet was resuspended in 1 mL of 10% sarcosine in 1X TEND, incubated for 1 h on ice, and centrifuged at 22 000 g for 30 min at 4°C. The pellet (P_0) was collected while the two supernatants were combined and centrifuged at 150 000 g for 2.5 h at 4°C. The new supernatant (S_0) was removed and collected for further analysis, while the pellet was rinsed with 50 μL of 100 mmol/L NaCl, 1% sulfobetaine (SB) 3–14, 1X TEND plus Complete® protease inhibitors, resuspended in 1 mL of the same buffer, and centrifuged at 180 000 g for 2 h at 20°C. The supernatant (S_1) was removed and collected, while the pellet was rinsed with 50 μL of 1X TMS (10 mmol/L Tris–HCl pH 7, 5 mmol/L MgCl$_2$, and 100 mmol/L NaCl) plus Complete®

protease inhibitors, resuspended in 600 μL of the same buffer containing 100 μg/mL Rnase A and incubated for 2 h at 37°C. The sample was then incubated with 5 mmol/L CaCl$_2$, 20 μg/mL Dnase I for 2 h at 37°C to stop the enzymatic digestion, EDTA was added to final concentration of 20 mmol/L, and the sample was mixed with an equal volume of 1X TMS, 1% SB 3–14. The sample was deposited gently on a small cushion of 1 mol/L sucrose, 100 mmol/L NaCl, 0.5% SB 3–14, and 10 mmol/L Tris–HCl pH 7.4, and centrifuged at 180 000 g for 2 h at 4°C. The supernatant (S_2) was collected while the pellet was rinsed with 50 μL of 0.5% SB 3–14, 1X PBS, resuspended in 100 μL of the same buffer by 10 × 5 s pulses of direct sonication with a Bandelin Sonopuls Ultrasonicator (Amtrex Technologies, Saint-Laurent, QC, Canada) at 90% power, and centrifuged at 180 000 g for 15 min at 37°C. The final supernatant (S_3) was collected while the pellet (P_3) was resuspended in 100 μL of 0.5% SB 3–14, 1X PBS. All the collected fractions were then subjected to western blotting using mAb 3F4.

Separation of soluble and insoluble PG14 by one-step ultracentrifugation

One mouse brain was homogenized in five volumes (w/v) of ice-cold PBS with EDTA-free Complete® protease inhibitors using a Teflon-glass homogenizer. The homogenate was centrifuged at 100 g for 30 s, and the post-nuclear supernatant was removed and centrifuged at 3200 g for 20 min. The pellet was then resuspended in 5 mL of homogenization buffer (1X PBS, 1% sodium deoxycholate, and 1% Triton X-100) plus EDTA-free Complete® protease inhibitors using a Wheaton glass Dounce homogenizer (10 strokes with pestle B), incubated on ice for 30 min, and further centrifuged at 180 000 g for 1 h. After centrifugation, the supernatant (soluble fraction) was collected, while the pellet was resuspended in 5 mL of homogenization buffer and sonicated (10 × 5 s at 90% power) (insoluble or aggregated fraction).

Immobilized metal affinity chromatography

The procedure we employed was a modification of one described elsewhere (Deleault *et al.* 2005). All procedures were performed at 4°C. Brain homogenates or fractionated PrP samples were pre-cleared with 200 μL of metal-free IMAC resin (Amersham Biosciences, Piscataway, NJ, USA), and then incubated with 200 μL of Cu^{2+}-IMAC resin on an end-over-end rotator for 2 h, and centrifuged for 1 min at 1000 g. Unbound PrP in the supernatant was precipitated with five volumes of methanol, and the beads were washed twice in 1 mL of Cu^{2+}-IMAC wash buffer (20 mmol/L 3-[N-Morpholino]propanesulfonic acid, pH 7.0, 0.15 mol/L NaCl, 10 mmol/L imidazole, and 1% Triton) plus EDTA-free Complete® protease inhibitors. Bound PrP was then eluted twice from the resin with 500 μL of Cu^{2+}-IMAC elution buffer (20 mmol/L 3-[N-Morpholino]propanesulfonic acid pH 7.5, 0.15 mol/L NaCl, 0.15 mol/L imidazole, and 1% Triton X-100) containing EDTA-free Complete® protease inhibitors.

NaPTA precipitation

Brain homogenates or fractionated PrP samples were mixed with a stock solution containing 4% NaPTA and 170 mmol/L MgCl$_2$ (pH 7.4), to obtain a final concentration of 0.2–0.3% NaPTA. Samples were incubated for 16 h at 37°C on a rocking platform, and then centrifuged at 13 000 g for 30 min at 25°C. Proteins in the pellet

fraction and the supernatant fraction (after methanol precipitation) were then subjected to western blotting.

Immunoprecipitation using PrP^C- and PrP^{Sc}-specific antibodies

To prepare agarose beads coated with mAbs 8H4 or 3F4, 400 μL of a 50% slurry of ImmunoPure Immobilized Protein A Plus (Pierce, Rockford, IL, USA) was incubated for 2 h with purified mAb (16 μg of IgG/μL of packed resin). Beads were recovered by centrifugation at 1000 *g* for 1 min, and washed twice with 1 mL of 200 mmol/L triethanolamine, pH 8.0. Antibodies were cross-linked to the beads by incubation for 30 min in 1 mL of 10 mmol/L dimethyl pimelimidate hydrochloride, 200 mmol/L triethanolamine, pH 8.0. The reaction was quenched by the addition of 50 μL of 1 mol/L Tris, pH 8.0, and beads were recovered by centrifugation at 1000 *g* for 1 min. Beads were then washed three times, once in 1X PBS, 1% Triton X-100, and twice in 1X PBS. Beads were resuspended in 200 μL of 1X PBS and stored at 4°C.

Immunoprecipitation of PrP with 3F4- or 8H4-coated beads was based on modification of a method described by Deleault *et al.* (2005). Brain homogenates or fractionated PrP samples were incubated with either 8H4- or 3F4-coated protein A-agarose beads prepared as above (50 μL of a 50% slurry), incubated end-over-end for 2 h, and centrifuged for 1 min at 1500 *g*. The supernatant containing the non-bound proteins was removed and proteins precipitated by methanol. The beads were washed once with 2 mL of Immunopure Gentle Ag/Ab Binding Buffer (Pierce), transferred to a clean microcentrifuge tube, and washed again in 1 mL of the same buffer. PrP was eluted from the washed beads with 200 μL of Immunopure Gentle Ag/Ab Elution Buffer (Pierce).

For immunoprecipitation assays involving mAb 15B3 (Prionics, Zurich, Switzerland), we followed the directions of the manufacturer, using the buffers supplied by them. 15B3 antibody was bound to magnetic Dynabeads coated with rat anti-IgM (Invitrogen, Carlsbad, CA, USA).

Protein misfolding cyclic amplification

Although the principle of PMCA remains the same as in the original publication (Saborio *et al.* 2001), we used a new, automated version of the assay (Saa *et al.* 2006). Tg(WT) brains were used as the source of PrP^C substrate. Ten percent (w/v) brain homogenates were prepared in conversion buffer (PBS containing NaCl 150 mmol/L, 1.0% Triton X-100, 4 mmol/L EDTA, plus EDTA-free Complete$^®$ protease inhibitors). The samples were clarified by centrifugation at 300 *g* for 30 s in a tabletop centrifuge. PG14^{Spon} or PG14^{RML} samples (either brain homogenates, or semi-purified P$_3$ fractions, see above) were mixed (1 : 200) with Tg(WT) brain homogenate and loaded into 0.2-mL PCR tubes. Tubes were positioned on an adaptor placed on the plate holder of a microsonicator (Model 3000; Misonix, Farmingdale, NY, USA). The sonicator was programmed to perform cycles of 30 min of incubation at 37°C followed by a 40 s pulse of sonication at 60% power. Tubes were incubated without shaking, immersed in the sonicator bath, and the entire microplate horn was kept inside an incubator at 37°C.

After completion of the PMCA reaction, 10 μL of each sample was diluted 1 : 10 in proteinase K (PK) digestion buffer (Tris–HCl 50 mmol/L pH 8.5, 150 mmol/L NaCl) and incubated with 10 μg/mL of PK at 37°C for 1 h on an end-over-end rotator prior to western blotting with anti-PrP antibody 8H4.

Western blotting

Total protein content in each sample was determined by bicinchoninic acid assay (Pierce). Protein samples were resuspended in 2X Laemmli sample buffer, heated at 95°C for 5 min, and resolved by sodium dodecyl sulfate–polyacrylamide gel electrophoresis using a 12% discontinuous gel. Proteins were electrophoretically transferred to polyvinylidene fluoride membranes, and the membranes were blocked for 10 min in 5% (w/v) non-fat milk in Tris-buffered saline containing Tween 20. After incubation with appropriate primary and secondary antibodies, signals were revealed using enhanced chemiluminescence (Amersham Biosciences), and were visualized by exposure to X-ray film. Anti-PrP antibodies 3F4 (Bolton *et al.* 1991) or 8H4 (Zanusso *et al.* 1998) were used to develop western blots, as indicated in the figure legends. In some cases, protein samples were enzymatically deglycosylated prior to western blotting by treatment with PNGase F (New England Biolab, Ipswich, MA, USA) for 16 h at 37°C following the manufacturer's instructions.

Brain sections from Tg(PrP–EGFP) mice

Animals were perfused intracardially with 60 mL of PBS followed by 40 mL of 4% paraformaldehyde 0.1 mol/L sodium phosphate buffer (pH 7.2). Brains were removed, immersed in the same fixative solution for 2 h, then transferred to 0.1 mol/L sodium phosphate buffer (pH 7.2) and stored at 4°C. Sagittal sections (60 μm) were cut using a vibratome (The Vibratome Company, St Louis, MO, USA), and were mounted on glass slides using Gel/Mount (Biomeda, Foster City, CA, USA). Sections were imaged using an LSM 510 META confocal microscope (Zeiss, Wetzlar, Germany).

Cultures of primary neurons from Tg(PrP–EGFP) mice

Cerebellar granule neurons were derived from 4-day-old pups according to methods described previously (Miller and Johnson 1996). Neurons were plated onto glass-bottom Petri dishes (Mattek, Ashland, MA, USA) using basal medium Eagle's containing 10% dialyzed fetal bovine serum, 25 mmol/L KCl, 2 mmol/L glutamine, and 50 μg/mL gentamycin. After 4 days in culture, cells were imaged in the living state using an LSM 510 META confocal microscope.

Results

Aggregated PG14^{Spon} and PG14^{RML} can be separated from soluble PG14 PrP by differential centrifugation

To characterize the biochemical properties of PG14^{Spon} and PG14^{RML}, we sought to purify these forms from the brains of uninoculated and RML scrapie-infected Tg(PG14) mice, respectively. For this purpose, we adopted a differential centrifugation procedure (Fig. 1a) that is typical of the ones used to purify PrP^{Sc} aggregates from scrapie-infected brain (Silveira *et al.* 2005). For comparison, we also applied the same procedure to brains from uninfected and RML-infected Tg(WT) mice.

We found that substantial amounts of PG14 PrP were recovered in the final pellet fraction (P$_3$) from both

Fig. 1 Aggregated PG14^{Spon} and PG14^{RML} can be separated from PG14^{Sol} by differential centrifugation. Brain homogenates from the following types of mice were fractionated by the scheme shown in (a): uninoculated transgenic (Tg)(PG14) (b); RML-infected Tg(PG14) (c); uninoculated Tg(wild-type, WT) (d); and RML-infected Tg(WT) (e) Fractions were subjected to western blotting using anti-PrP antibody 3F4. Soluble PG14 (PG14^{Sol}) is found in the S$_0$ fraction from both uninfected and RML-infected Tg(PG14) brains (lane 2 of panels b and c), aggregated PG14^{Spon} in the P$_3$ fraction from uninoculated Tg(PG14) brain (lane 6 of panel b), and aggregated PG14^{RML} in the P$_3$ fraction from RML-infected Tg(PG14) brain (lane 6 of panel c). Molecular size markers are given in kilodaltons. In this and all subsequent figures, results have been reproduced in at least three independent experiments, each using a different mouse brain.

uninfected and RML-infected Tg(PG14) brains (Fig. 1b and c; lane 6). Similarly, most of the PrP in RML-infected Tg(WT) brain was found in the P$_3$ pellet (Fig. 1e, lane 6). Based on silver staining of sodium dodecyl sulfate–polyacrylamide gel electrophoresis gels, we estimate that the

differential centrifugation procedure significantly enriched both PG14^{Spon} and PG14^{RML} aggregates, with the final level of purity in the P$_3$ fraction being 20–40% for both samples (data not shown). We noted that a small proportion (< 5%) of the PrP from the brains of uninoculated Tg(WT) mice was

recovered in the P_3 fraction (Fig. 1d, lane 6), in agreement with previously published results (Yuan *et al.* 2006).

We also consistently recovered a proportion of the PG14 PrP from both infected and uninfected brains in the S_0 fraction (Fig. 1b and c; lane 2). The S_0 fraction is where most ($\sim$95%) of the PrP^C from uninfected Tg(WT) brains was found (Fig. 1d, lane 2), and where a small proportion (10–20%) of the PrP from RML-infected Tg(WT) brains was also recovered (Fig. 1e, lane 2). The proportion of PG14 PrP in the S_0 fraction was generally higher in uninfected than in infected brains ($\sim$40% vs. $\sim$20%). These observations indicate that a subpopulation of PG14 molecules in both kinds of brains remain soluble. We will refer to this soluble form as PG14^{Sol}, to distinguish it from the aggregated forms found in the P_3 fractions which we will continue to designate as PG14^{Spon} and PG14^{RML}. PG14^{Sol} shows the same sensitivity to PK digestion as PrP^C from Tg(WT) brain (data not shown).

The evidence to be presented below indicates that PG14^{Sol} from both uninoculated and scrapie-infected brains has the biochemical properties of WT PrP^C. In contrast, PG14^{Spon} and PG14^{RML} possess many of the biochemical properties of PrP^{Sc}. For these experiments, aggregated forms of PG14^{Spon} and PG14^{RML} were separated from PG14^{Sol} by a one-step ultracentrifugation procedure in which brain lysates were spun at 180 000 *g*. The supernatant fraction (containing PG14^{Sol}) and the pellet fraction (containing aggregated PG14^{Spon} and PG14^{RML}) were then analyzed separately. We obtained similar results when we utilized the purification scheme outlined in Fig. 1a in which PG14^{Sol} was recovered in the S_0 fraction and PG14^{Spon} and PG14^{RML} in the P_3 fraction (data not shown).

PG14^{Sol}, but not aggregated PG14^{Spon} or PG14^{RML}, bind to Cu^{2+}–IMAC resin

It has been reported that PrP^{Sc}, in contrast to PrP^C, is unable to bind copper immobilized on a chromatography matrix (Shaked *et al.* 2001). To test the copper binding of different forms of PG14 PrP, samples prepared from infected and uninfected brain were incubated with Cu^{2+}-IMAC resin, followed by western blot analysis of PrP in the bound and unbound fractions.

We found that insoluble aggregates of PG14^{Spon} and PG14^{RML}, like PrP^{Sc} from infected Tg(WT) mice, are unable to bind efficiently to the Cu^{2+}-IMAC resin, and are recovered predominantly in the unbound fraction (Fig. 2, compare lanes 3–4, 7–8, and 15–16). In contrast, soluble PG14 PrP (PG14^{Sol}) from both infected and non-infected animals bound efficiently to the resin, as did soluble PrP^C from uninfected Tg(WT) brain (Fig. 2, compare lanes 1–2, 5–6, and 9–10). Because the octarepeat region of PrP makes an important contribution to binding of copper ions (Stöckel *et al.* 1998; Kramer *et al.* 2001; Millhauser 2007) these results indicate that the extended octarepeats in PG14^{Spon} and PG14^{RML} are likely to be sterically masked, as is the case for PrP^{Sc}.

Aggregated PG14^{Spon} and PG14^{RML} are precipitated by NaPTA

Sodium phosphotungstic acid has been found to be relatively selective in precipitating PrP^{Sc}, but not PrP^C (Safar *et al.* 1998). This phenomenon has been used to concentrate PrP^{Sc} from tissue samples for western blotting (Wadsworth *et al.* 2001). We found that insoluble PG14^{Spon} and PG14^{RML} are efficiently precipitated by NaPTA, similar to PrP^{Sc} from
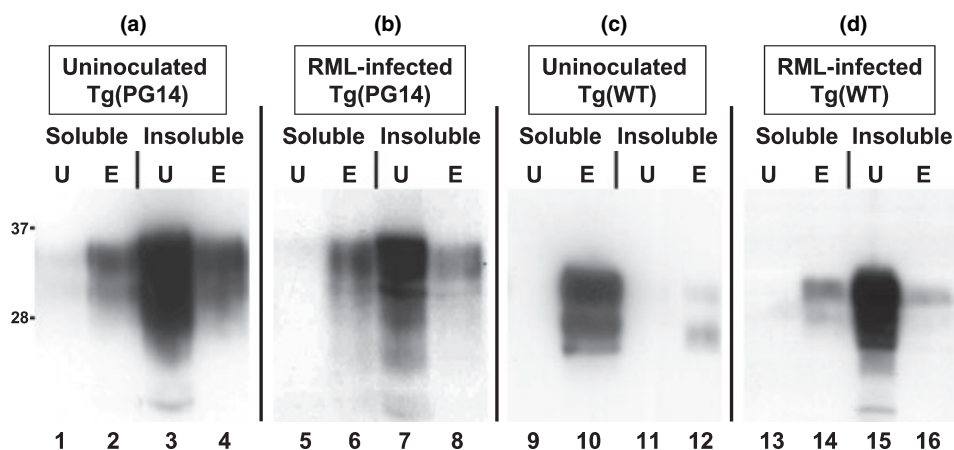

Fig. 2 PG14^{Sol}, but not aggregated PG14^{Spon} or PG14^{RML}, bind to Cu^{2+}-immobilized metal affinity chromatography (IMAC) resin. Soluble and insoluble fractions of PrP were obtained by one-step ultracentrifugation of brain homogenates from the following mice: (a) uninoculated transgenic (Tg)(PG14) (lanes 1–4); (b) RML-infected Tg(PG14) (lanes 5–8); (c) uninoculated Tg(wild type, WT) (lanes 9–12); (d) RML-infected Tg(WT) (lanes 13–16). Soluble fractions (lanes 1, 2, 5, 6, 9, 10, 13, and 14) and insoluble fractions (lanes 3, 4, 7, 8, 11, 12, 15, and 16) were incubated with Cu^{2+}-IMAC resin. The supernatant containing unbound proteins was then collected (U lanes), and the beads were eluted with buffer containing 0.15 mol/L imidazole (E lanes). PrP in each sample was detected by western blotting with anti-PrP antibody 3F4.
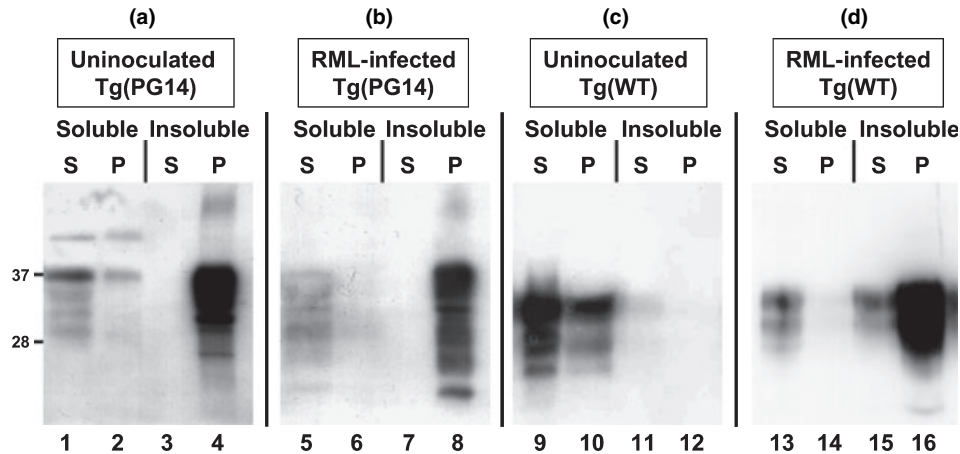
Fig. 3 Aggregated PG14^{Spon} and PG14^{RML} are precipitated by NaPTA. Soluble and insoluble fractions of PrP were obtained by one-step ultracentrifugation of brain homogenates from the following mice: (a) uninoculated transgenic (Tg)(PG14) (lanes 1–4); (b) RML-infected Tg(PG14) (lanes 5–8); (c) uninoculated Tg(WT) (lanes 9–12); (d) RML-infected Tg(WT) (lanes 13–16). Soluble fractions (lanes 1, 2, 5, 6, 9, 10, 13, and 14) and insoluble fractions (lanes 3, 4, 7, 8, 11, 12, 15, and 16) were treated with NaPTA (0.2–0.3% final concentration). After centrifugation, PrP in supernatant fractions (S lanes) and pellet fractions (P lanes) was detected by western blotting with anti-PrP antibody 3F4.

infected Tg(WT) brain (Fig. 3, compare lanes 3–4, 7–8, and 15–16). In contrast, PG14^{Sol} from both infected and uninfected brain was not precipitated as effectively, as was the case for PrP^C from uninoculated Tg(WT) brain (Fig. 3, compare lanes 1–2, 5–6, and 9–10). These results indicate that, in terms of their propensity to be precipitated by NaPTA, PG14^{Spon} and PG14^{RML} aggregates resemble PrP^{Sc}, while PG14^{Sol} resembles PrP^C.

Aggregated PG14^{Spon} and PG14^{RML} are not recognized by antibodies 8H4 and 3F4

Antibody epitopes in several regions of the PrP molecule are known to become inaccessible upon conversion from PrP^C to PrP^{Sc} (Safar et al. 1998; Pan et al. 2004). To determine the epitope availability of different forms of PG14 PrP, we tested the binding of two PrP-specific mAbs, 8H4 and 3F4, whose epitopes encompass PrP residues 175–185 and 108–111, respectively (Bolton et al. 1991; Pan et al. 2004). Samples were incubated under non-denaturing conditions with protein A-agarose beads cross-linked to either 8H4 or 3F4 antibodies, and PrP in the bound and unbound fractions was revealed by western blotting with 3F4 antibody.

We found that aggregated PG14^{Spon} and PG14^{RML} were not efficiently immunoprecipitated by 8H4, similar to PrP^{Sc} from infected Tg(WT) brain (Fig. 4, compare lanes 3–4, 7–8, and 15–16). In contrast, most of the PG14^{Sol} from both infected and uninfected Tg(PG14) brain, as well as the majority of PrP^C from uninfected Tg(WT) brain, were recognized by 8H4 (Fig. 4, compare lanes 1–2, 5–6, and 9–10). Similar results were obtained using beads cross-linked to 3F4 antibody (data not shown). These results demonstrate that epitopes in the C-terminal half and central region of PrP are

masked in PG14^{Spon} and PG14^{RML}, as they are in PrP^{Sc}. In contrast, these epitopes are accessible in PG14^{Sol} and PrP^C.

Parallel to what we have observed in immunoprecipitation experiments, 8H4 and 3F4 antibodies do not efficiently label PG14^{Spon} and PG14^{RML} in paraffin-embedded sections of brain without antigen retrieval techniques (data not shown). However, a low level of staining similar in distribution to PrP^C is detectable, presumably corresponding to the presence of PG14^{Sol}. We have utilized the selective recognition of PG14^{Sol} by 8H4 and 3F4 antibodies to immunopurify this form from brain to ~75% purity (data not shown) using a previously published procedure (Deleault et al. 2005).

Aggregated PG14^{Spon} and PG14^{RML}, but not PG14^{Sol}, are recognized by mAb 15B3

To further characterize the structural properties of the different forms of PG14 PrP, we performed immunoprecipitation assays with mAb 15B3, which has been reported to selective recognize PrP^{Sc} and not PrP^C (Korth et al. 1997). As in the previous experiments, samples were first subjected to ultracentrifugation to separate soluble and aggregated forms of PG14 PrP.

First, we confirmed the specificity of 15B3 by demonstrating its ability to immunoprecipitate PrP^{Sc} present in the insoluble fraction from RML-infected Tg(WT) brain (Fig. 5b, lane 4). Insoluble PG14^{RML} from scrapie-infected brain was also precipitated by 15B3 (Fig. 5b, lane 8). Surprisingly, however, the antibody also recognized insoluble PG14^{Spon} (Fig. 5b, lane 6), even though this form is derived from uninfected brain and is not infectious like PrP^{Sc} (see below). 15B3 was highly specific for aggregated forms of PrP (Fig. 5a and b): it did not immunoprecipitate soluble
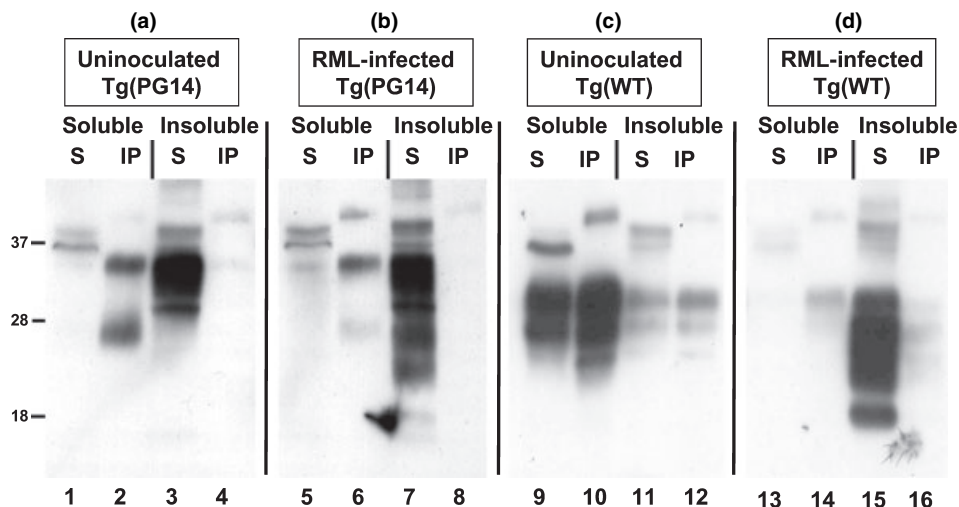
Fig. 4 Aggregated PG14^{Spon} and PG14^{RML} are not recognized by 8H4 antibody. Soluble and insoluble fractions of PrP were obtained by one-step ultracentrifugation of brain homogenates from the following mice: (a) uninoculated transgenic (Tg)(PG14) (lanes 1–4); (b) RML-infected Tg(PG14) (lanes 5–8); (c) uninoculated Tg(WT) (lanes 9–12); (d) RML-infected Tg(WT) (lanes 13–16). Soluble fractions (lanes 1, 2, 5, 6, 9, 10, 13, and 14) and insoluble fractions (lanes 3, 4, 7, 8, 11, 12, 15, and 16) were incubated with protein A-agarose beads coated with MAb 8H4. PrP bound to the beads (IP lanes) and remaining in the supernatant (S lanes) was then detected by western blotting with anti-PrP antibody 3F4. A 26 kDa band, which is soluble and immunoprecipitated by 8H4 in uninoculated Tg(PG14) brains (lane 2), but is insoluble and non-reactive with 8H4 in infected Tg(PG14) brains (lane 7), most likely represents the glycosylated C2 proteolytic fragment of PrP (see also Fig. 7b).

forms (even when present in large excess), including PrP^C in uninfected brain (lane 1), PG14^{Sol} in both infected and uninfected brain (lanes 5 and 7), and residual soluble PrP in RML-infected Tg(WT) brain (lane 3).

Collectively, these results indicate that aggregated PG14^{Spon} is structurally distinct from PG14^{Sol} and PrP^C, and shares conformational features with infectious PG14^{RML} and PrP^{Sc}.

PG14^{RML}, but not PG14^{Spon}, supports *in vitro* misfolding of PrP^C by PMCA

We previously showed that PG14^{RML}, but not PG14^{Spon}, is infectious in animal transmission studies using Tg(WT) as well as other host mice (Chiesa *et al.* 2003). To further assess the ability of these forms to propagate their conformations to WT PrP, we used PMCA technology (Saborio *et al.* 2001; Castilla *et al.* 2005; Saa *et al.* 2006). In this method, a brain homogenate containing PrP^C substrate is seeded with a sample of PrP^{Sc}, and the mixture is then subjected to repeated rounds of sonication and incubation, followed by PK digestion and western blotting to assess the amount of protease-resistant PrP generated.

Reactions were seeded with aggregated PG14^{RML} and PG14^{Spon}, either in the form of the semi-purified P$_3$ fraction (see Fig. 1, lane 6; Fig. 6), or present in crude brain homogenates (not shown). Seeds were diluted into Tg(WT) brain homogenate and then subjected to 0, 10, or 40 cycles of sonication. After amplification, each sample was digested

with 10 µg/mL of PK, and PrP was visualized by western blotting using antibody 8H4. We observed that PG14^{RML} seeded formation of protease-resistant PrP that was detectable after 20 cycles, with the amount increasing further after 40 cycles (Fig. 6, lanes 7 and 8). In contrast, PG14^{Spon} lacked detectable seeding activity, even after 40 cycles (Fig. 6, lanes 3 and 4). Control reactions without sonication did not produce any protease-resistant PrP (Fig. 6, lanes 2 and 6). These results demonstrate that aggregated PG14^{RML}, but not PG14^{Spon}, is able to propagate its conformation *in vitro*.

PG14^{Spon} does not co-aggregate with WT PrP or the C2 fragment

Propagation of PrP^{Sc} is thought to involve two distinct steps: binding of the PrP^{Sc} seed to the PrP^C substrate, followed by conformational conversion of PrP^C (Caughey 2001). To determine whether the inability of PG14^{Spon} to propagate its conformation to WT PrP either *in vitro* (above) or *in vivo* (Chiesa *et al.* 2003) is due to a defect in the binding step, we analyzed co-aggregation of PG14 PrP with WT PrP in uninfected, doubly Tg(PG14/WT) mice that express both PrP forms. Brain lysates from these animals were subjected to ultracentrifugation and the amount of WT and PG14 PrP in the pellet and supernatant fractions was analyzed by western blotting. We found that while PG14 PrP was partially insoluble, WT PrP remained fully soluble, even in terminally ill, older animals (Fig. 7a, lanes 1, 3, and 5). This observa-
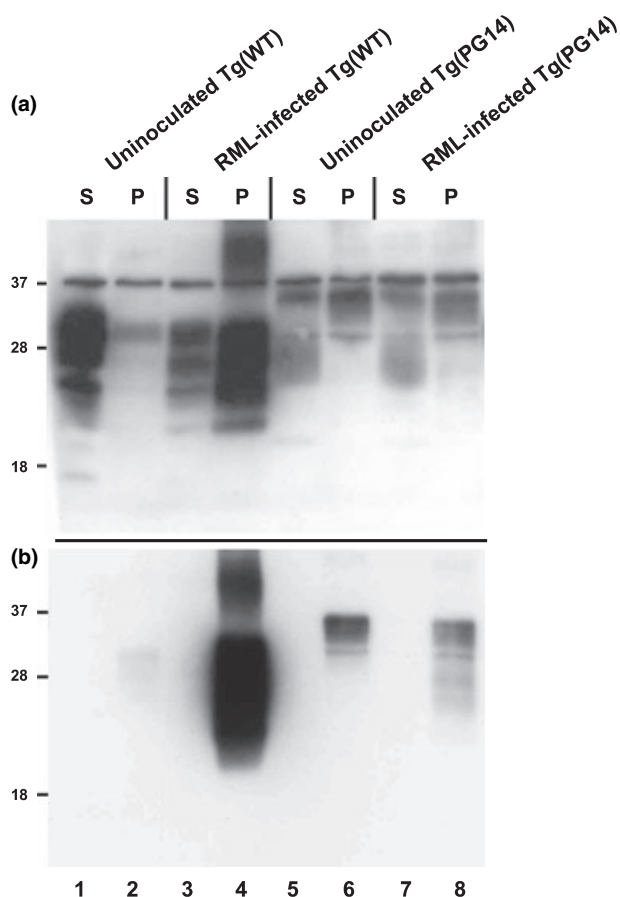
Fig. 5 Aggregated PG14[Spon] and PG14[RML], but not PG14[Sol] are recognized by mAb 15B3. Soluble and insoluble fractions of PrP were obtained by one-step ultracentrifugation of brain homogenates from uninoculated transgenic (Tg)(wild-type, WT) mice (lanes 1 and 2), RML-infected Tg(WT) mice (lanes 3 and 4), uninoculated Tg(PG14) mice (lanes 5 and 6), or RML-infected Tg(PG14) mice (lanes 7 and 8). Soluble fractions (S lanes: 1, 3, 5, and 7) and insoluble fractions (P lanes: 2, 4, 6, and 8) were either (a) directly immunoblotted with 3F4 antibody; or (b) first incubated with 15B3 bound to anti-IgM-coupled Dynabeads, after which proteins bound to the Dynabeads were subjected to western blotting with 3F4 antibody.

tion indicates that PG14[Spon] aggregates are not capable of binding to WT PrP.

We also studied the binding of PG14 PrP aggregates to an endogenously produced, C-terminal fragment of PrP designated C2 (Chen *et al.* 1995). This fragment, which is cleaved near residue 90 by endogenous proteases, corresponds to the protease-resistant PrP 27–30 fragment that is produced experimentally by digestion with PK. Of relevance here, the C2 fragment has been found to co-aggregate with PrP[Sc] in the brains of Creutzfeldt-Jakob disease patients (Chen *et al.* 1995). Brain lysates from uninfected and RML-infected Tg(PG14) mice, as well as uninfected Tg(WT) control mice, were subjected to ultracentrifugation. Supernatant and pellet fractions were then treated with PNGase to remove N-linked oligosaccharides, and so facilitate separation of full-length PrP and the C2 fragment. As expected, in Tg(WT) brains both full-length PrP[C] (27 kDa) as well as C2 (20 kDa) were present entirely in the supernatant fraction (Fig. 7b, lanes 1 and 2). In both uninfected and scrapie-infected Tg(PG14) brains, full-length PG14 PrP (33 kDa) partitioned mainly into the pellet, with a small amount (corresponding to PG14[Sol]) in the supernatant (Fig. 7b, lanes 3 and 4, and 5 and 6). Significantly, however, the C2 fragment was found entirely in the supernatant in uninfected Tg(PG14) brain, but entirely in the pellet in RML-infected Tg(PG14) brain (Fig. 7b, lanes 3 and 6). As the C2 fragment lacks the N-terminal half of PrP, including the expanded octapeptide repeats, these results demonstrate that aggregates of PG14[Spon] are unable to bind proteolytically derived PrP molecules lacking the repeat domain. The presence of both full-length PG14 PrP and C2 in the pellet fraction from infected brains may indicate that PG14[RML] aggregates bind to C2 as part of the conversion process.

PG14[Spon] does not co-aggregate with EGFP-tagged WT PrP in brain sections and cultured neurons

We have shown recently that a PrP-EGFP fusion protein expressed in Tg mice specifically binds to and labels deposits of PrP[Sc] derived from co-expressed endogenous PrP (Barmada and Harris 2005). To test whether PrP-EGFP can also interact with PG14[Spon] aggregates, we analyzed brain sections and cultured cerebellar granule neurons from doubly Tg mice co-expressing PG14 PrP and WT PrP-EGFP. As controls, we also examined samples from singly Tg mice expressing either WT or PG14 versions of PrP-EGFP.

As reported previously (Barmada *et al.* 2004), cerebellar sections from Tg(WT PrP-EGFP) mice show a diffuse fluorescent signal throughout the molecular layer and in islands corresponding to glomeruli in the granule cell layer (Fig. 8a). In cultured granule neurons derived from these animals, fluorescence is uniformly distributed on the surface of neurites (Fig. 8d). In contrast, PG14 PrP-EGFP in both brain tissue and cultured neurons are distributed in a much more punctate fashion, reflecting the propensity of this protein to aggregate (A. Z. Medrano, S. J. Barmada, E. Biasini and D. A. Harris; paper submitted). Cerebellar sections from Tg(PG14 PrP-EGFP) mice show prominent puncta of fluorescence, particularly in the molecular layer (Fig. 8b). Cultured granule neurons from these mice display numerous, discrete aggregates of fluorescence along their neurites, with little surface fluorescence (Fig. 8e). Significantly, in brain sections and granule neurons from doubly Tg(WT PrP-EGFP/PG14) mice, the PrP signal was mainly diffuse, similar to the situation in singly Tg(WT PrP-EGFP) mice (Fig. 8c and f). These results indicate that WT PrP-EGFP does not bind to and label PG14[Spon] aggregates in the same way as it does PrP[Sc] aggregates in scrapie-infected mice (Barmada and Harris 2005).
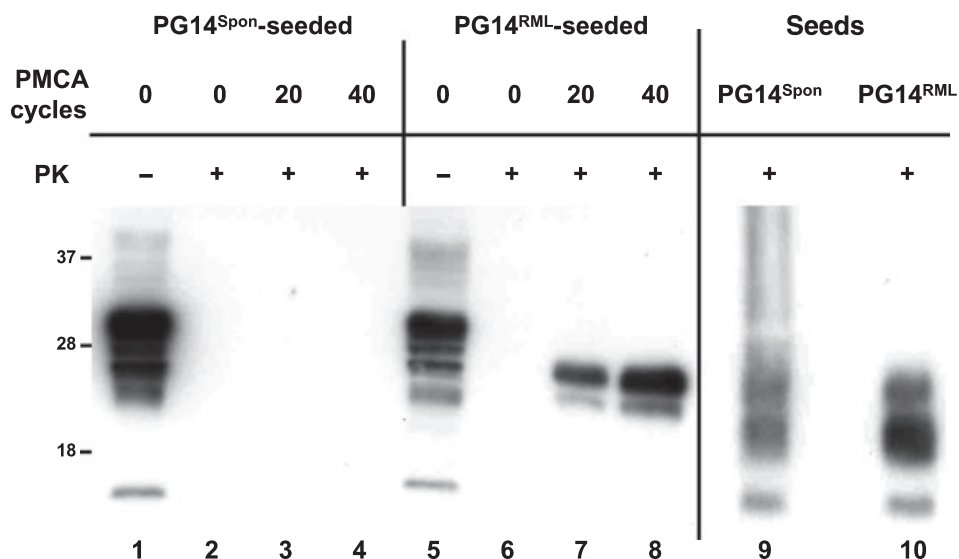
Fig. 6 PG14[RML], but not PG14[Spon], supports *in vitro* misfolding of PrP[C] by PMCA. Partially purified aliquots of PG14[Spon] (1–4) or PG14[RML] (5–8) present in the P₃ fraction (see Fig. 1, lane 6) were mixed with transgenic (Tg) (wild-type, WT) brain homogenate. Mixtures were either rapidly frozen (lanes 1 and 2, and 5 and 6), or were subjected to 20 cycles (lanes 3 and 7) or 40 cycles (lanes 4 and 8) of sonication/incubation. Samples were then subjected to proteinase K (PK) digestion (lanes 2–4 and 6–8), or were left undigested (lanes 1 and 5). Lanes 9 and 10 show PK digestion of the partially purified PG14[Spon] and PG14[RML] samples added to the PMCA reaction (10X larger amounts than used in lanes 1–8), provided to illustrate the digestion pattern of the seeds. All samples were subjected to western blotting with 8H4 antibody.

We previously reported that expression of WT PrP-EGFP in *Prn-p+/+* mice significantly prolonged the incubation time after scrapie inoculation, compared to non-Tg *Prn-p+/+* mice (Barmada and Harris 2005). This phenomenon reflects a dominant-negative effect of PrP-EGFP or formation of PrP[Sc] derived from endogenous PrP. In contrast, we observed that the presence of PrP-EGFP did not alter the age at symptom onset in Tg(WT PrP-EGFP/PG14) mice, compared with Tg(PG14) mice lacking PrP-EGFP (321 ± 21 days vs. 317 ± 28 days, respectively). This result provides additional evidence that PG14[Spon], unlike PrP[Sc], does not physically interact with WT PrP-EGFP.

Discussion

This study was undertaken with the aim of further characterizing the biochemical properties of PG14[Spon] and PG14[RML], two forms of mutant PrP with a nine-octapeptide repeat insertion found in uninoculated and scrapie-infected Tg(PG14) mice, respectively. PG14[Spon] is weakly PK-resistant, but it is not infectious and is therefore distinct from PrP[Sc]. PG14[RML] is highly PK-resistant and infectious, and so is equivalent to PrP[Sc].

Strikingly, we find that although PG14[Spon] and PG14[RML] differ markedly in terms of infectivity, aggregates of these proteins behave similarly in a variety of biochemical tests that assay protein conformation or oligomeric state (Table 1).

In contrast, PG14[Sol], a soluble form of PG14 PrP found in both uninoculated and RML-infected Tg(PG14) brains, exhibits properties of PrP[C] in these assays (Table 1). Although PG14[Spon] and PG14[RML] are biochemically similar, we show here that only PG14[RML] is capable of propagating its conformation to WT PrP in an *in vitro* PMCA reaction, consistent with its infectivity in animal bioassays (Chiesa *et al.* 2003) (Table 2). In addition to being catalytically inactive in the PMCA assay, PG14[Spon] is unable to bind WT PrP or the C2 fragment in co-sedimentation experiments, or to re-distribute PrP-EGFP in fluorescence microscopy experiments (Table 2).

Taken together, these results further refine our understanding of the molecular properties of toxic and infectious forms of PrP, and they prompt a re-interpretation of assays designed to detect PrP[Sc] based exclusively on biochemical properties or specific antibody reactivity.

Similarities between PG14[Spon] and PG14[RML]

One of the principal conclusions to emerge from this work is the striking similarity between PG14[Spon] and PG14[RML] aggregates in their biochemical properties and immunological reactivity (Table 1). In contrast to PrP[C] and soluble PG14 (PG14[Sol]), both PG14[Spon] and PG14[RML] fail to bind to Cu^{2+}-IMAC resin, and both are precipitable by NaPTA. In addition, both PG14[Spon] and PG14[RML] react poorly in the native state with several different monoclonal antibodies recognizing distinct parts of the PrP molecule, including 3F4
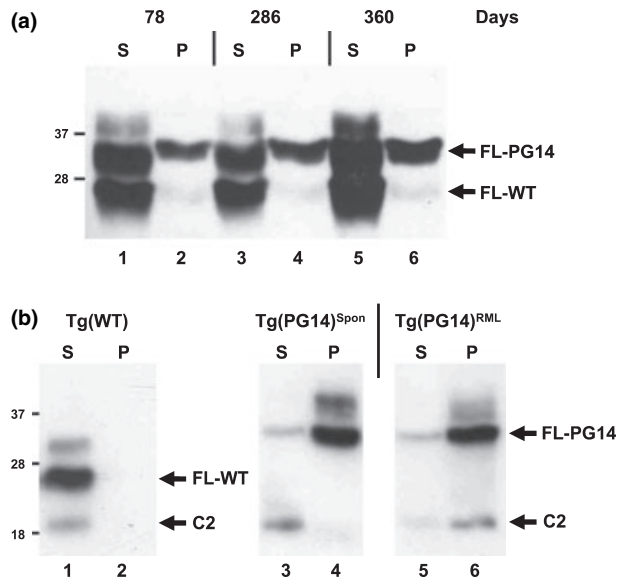
Fig. 7 PG14^Spon does not co-aggregate with WT PrP or the C2 fragment. (a) Brain homogenates from bigenic Tg(PG14/WT) mice were separated into soluble (S lanes) and insoluble fractions (P lanes) by one-step ultracentrifugation. Proteins in each fraction were deglycosylated with PNGase F prior to western blotting to facilitate separation of PG14 from WT PrP. Blots were developed with N terminally directed antibody P45–66, which detects full-length (FL) forms of both PG14 and WT PrP (indicated by the arrows to the right of lane 6). (b) Brain homogenates from transgenic (Tg)(WT) mice (lanes 1 and 2), uninoculated Tg(PG14) mice (lanes 3 and 4) and RML-infected Tg(PG14) mice (lanes 5 and 6) were separated into soluble (S lanes) and insoluble fractions (P lanes) by one-step ultracentrifugation. Proteins in each fractions were then subjected to PNGase treatment followed by western blotting using 3F4 antibody, which detects both FL WT and PG14 PrP, as well as the C2 fragment (indicated by arrows).

and 8H4 (this work), as well as P45–66 (Chiesa *et al.* 2003). Finally, both forms are efficiently recognized by 15B3, a mAb that recognizes PrP^Sc but not PrP^C.

These shared operational properties are likely to reflect common structural features of PG14^Spon and PG14^RML. Cu^{2+}-IMAC binding depends, at least in part, on accessibility of the histidine-containing octapeptide repeats in the N-terminal half of PrP (Stöckel *et al.* 1998; Kramer *et al.* 2001; Millhauser 2007). NaPTA precipitation is thought to involve electrostatic interactions between anionic polyoxometalate complexes and a positively charged cleft present in aggregated PrP molecules (Lee *et al.* 2005). Lack of reactivity with 3F4, 8H4, and P45–66 presumably reflects inaccessibility of the corresponding linear epitopes (residues 108–111, 175–185, and 45–66, respectively). Reactivity with 15B3 has been reported to depend on a conformational epitope comprised of three non-contiguous segments of the PrP sequence (residues 142–148, 162–170, and 214–226) (Korth *et al.* 1997). Of note, 15B3 has been found to recognize weakly PK-resistant, aggregated PrP from the brains of Tg

mice expressing a Gerstmann-Sträussler-Scheinker disease-related P101L mutation (Nazor *et al.* 2005), similar to the situation for PG14^Spon.

Taken together, our results indicate that there are important structural similarities between PG14^Spon and PG14^RML, despite the fact that latter is infectious while the former is not. What are these similarities? One feature shared by these two forms is that both are aggregated. Thus, oligomeric forms of PrP, whether or not they are infectious, may display common conformational motifs that distinguish them from monomeric PrP^C. For example, oligomerization could create new structural interfaces and/or obscure existing epitopes, resulting in altered recognition by antibodies, as well as by ligands such as NaPTA and Cu^{2+} ions. In fact, our own recent studies suggest that antibody 15B3, as well as motif-grafted antibodies (Moroncini *et al.* 2004; Solforosi *et al.* 2007), recognize common conformational epitopes in multiple aggregated forms of PrP, both infectious and non-infectious (E. Biasini, M. E. Seegulam, B. N. Patti, L. Solforosi, A. Z. Medrano, H. M. Christensen, A. Senatore, R. Chiesa, R. A. Williamson and D. A. Harris; paper submitted).

Another conformational feature that is likely to be shared by both PG14^Spon and PG14^RML is an increased proportion of β-sheet structure. It is well known that experimentally induced conversion of PrP from α-helical to β-sheet-rich forms is accompanied by oligomerization of the protein (Swietnicki *et al.* 2000; Baskakov *et al.* 2002; Surewicz *et al.* 2006; Baskakov and Breydo 2007). Thus, PG14^Spon and PG14^RML may both represent β-rich oligomers or polymers, with the β-sheet structure endowing these assemblies with similar reactivities in the biochemical assays we have employed here.

Differences between PG14^Spon and PG14^RML

The primary property that distinguishes PG14^Spon from PG14^RML is the infectivity of the latter, as defined in both animal transmission experiments and *in vitro* assays. In addition, PG14^RML is significantly more protease resistant than PG14^Spon. What, then, are the structural features that distinguish PG14^Spon from PG14^RML, and endow the latter with infectivity? In an earlier study, we reported that aggregates of PG14^RML were larger than those of PG14^Spon based on sucrose gradient centrifugation, and were less readily dissociated by urea (Chiesa *et al.* 2003). Based on these observations, we suggested that PG14^Spon and PG14^RML differed in the quaternary structures characterizing the organization of the subunits within these two kinds of aggregates. Thus, RML inoculation may seed the growth of PG14 PrP polymers that have a different size or morphology compared with those that form spontaneously in uninfected brain.

Silveira *et al.* (2005) have recently identified what they refer to as the most infectious units of PrP^Sc, corresponding to an oligomer composed of 14–28 PrP molecules. Strik-

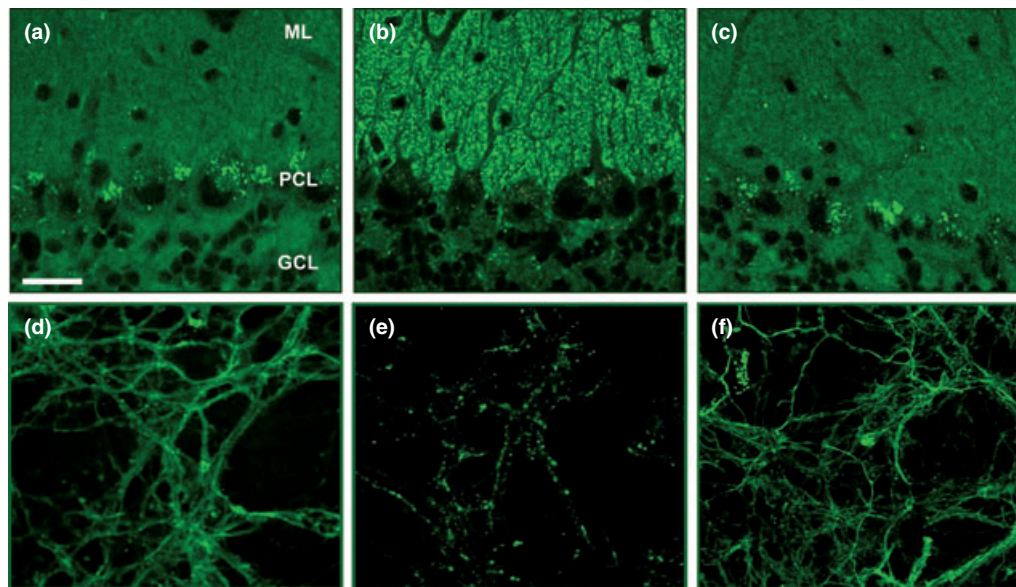**Fig. 8** PG14^Spon does not co-aggregate with EGFP-tagged WT PrP in brain sections (a–c) and cultured neurons (d–f). (a) Cerebellar section from a mouse expressing WT PrP-EGFP shows a relatively uniform, diffuse fluorescence in all layers of the cerebellum, with the exception of some auto-fluorescent dots in the Purkinje cell layer. (b) In contrast, a cerebellar section from a mouse expressing PG14 PrP-EGFP displays bright, fluorescent puncta throughout the molecular layer and to a lesser extent in the granule cell layer. (c) Cerebellar section from a mouse co-expressing WT PrP-EGFP and PG14 PrP displays a uniform, diffuse distribution of fluorescence, similar to panel (a) Abbreviations in panel (a) are: ML, molecular layer; PC, Purkinje cell layer; GCL, granule cell layer. Cerebellar granule neurons were cultured from mice expressing WT PrP-EGFP (d), PG14 PrP-EGFP (e), or both WT PrP-EGFP and PG14 PrP (f). WT PrP-EGFP uniformly coats the surface of neurites (d), while PG14 PrP-EGFP is distributed in aggregates within the neurites (e). Cultures co-expressing WT PrP-EGFP and PG14 PrP (f) show a uniform pattern of fluorescence, similar to (d). Scale bar in (a) (applicable to all panels) = 20 μm.

ingly, this is the same oligomer size that we have previously reported for non-infectious PG14^Spon (Chiesa *et al.* 2003). This comparison suggests that differences in size alone may not fully explain why PG14^RML aggregates are infectious while PG14^Spon aggregates are not. Consistent with this conclusion, there are several reports of 'protease-sensitive' forms of PrP^Sc that have a smaller oligomeric size than conventional, protease-resistant PrP^Sc, but which are nevertheless infectious (Safar *et al.* 1998; Tzaban *et al.* 2002; Pastrana *et al.* 2006). Thus, a relatively small particle size and low protease resistance are not incompatible with propagation of infectivity.

It has also been reported that in both yeast (Tanaka *et al.* 2006) and mammals (Legname *et al.* 2006) there is an inverse correlation between the efficiency with which a prion strain propagates and its structural stability (as measured, for example, by resistance to shearing or denaturation by guanidine hydrochloride). In these studies, less stable prion strains were found to propagate more rapidly, possibly because their polymers were more easily fragmented. However, this correlation would also not explain the lack of infectivity of PG14^Spon, whose oligomeric structure appears to be less stable than that of PG14^RML, as judged by greater susceptibility to disruption by chaotropic agents (Chiesa *et al.* 2003).

Studies of the folding and aggregation characteristics of purified, recombinant PrP provide a precedent for the existence of multiple types of PrP oligomer which differ in their degree of infectivity. In particular, Baskakov *et al.* have shown that PrP can adopt, in addition to its native, α-helical monomeric form, two non-native, β-rich forms: a β-oligomer and an amyloid fibril (Baskakov *et al.* 2002; Baskakov 2004; Baskakov and Breydo 2007). The β-oligomer consisted of approximately eight PrP molecules, while the amyloid fibril was much larger and displayed a variety of fibrillar morphologies in electron micrographs. Kinetic data suggested that β-oligomers were not on the pathway of amyloid formation and were not a substructure in the assembling fibrils. It has been reported recently that a subpopulation of amyloid fibrils formed from recombinant PrP are infectious, based on their ability to seed polymerization of monomeric PrP *in vitro* (Baskakov 2004) and to induce disease upon inoculation of Tg mice expressing high levels of PrP (Legname *et al.* 2004). In contrast, β-oligomers are considered to be non-infectious, although they are toxic to cultured cells (Novitskaya *et al.* 2006). An intriguing possibility is that PG14^Spon represents an aggregation state similar to the β-oligomer, while PG14^RML is comparable to an amyloid fibril. This suggestion is compatible with the sizes we have measured previously for PG14^Spon and

Table 1 Biochemical properties of PG14 forms, PrP^C, and PrP^{Sc}. The cartoon at the top of table shows a schematic of the hypothetical structure of each species. We envision that PG14^{Sol} serves as a common precursor to both PG14^{Spon} and PG14^{RML}. In uninoculated mice, PG14^{Sol} spontaneously aggregates into small oligomers; in infected mice, RML PrP^{Sc} seeds formation of larger polymers

	PrP^C	PG14^{Sol}	PG14^{Spon}	PG14^{RML}	PrP^{Sc}
Aggregated (detergent-insoluble)	No	No	Yes	Yes	Yes
PK resistance	No	No	5 µg/mL[*]	>100 µg/mL[*]	>100 µg/mL
Cu^{2+}-IMAC binding	Yes	Yes	No	No	No
NaPTA precipitation	No	No	Yes	Yes	Yes
PrP^C epitopes masked (3F4, 8H4, P45-66 *)	No	No	Yes	Yes	Yes
Recognized by 'PrP^{Sc}-specific' Abs (15B3, motif-grafted [†])	No	No	Yes	Yes	Yes

PK, proteinase K; IMAC, immobilized metal affinity chromatography; NaPTA, sodium phosphotungstic acid; Abs, antibodies; PG14, nine-octapeptide insertional mutation in prion protein (PrP); PrP^C, cellular PrP; PrP^{Sc}, scrapie isoform of PrP; PG14^{Sol}, soluble (non-aggregated) form of PG14 PrP; PG14^{Spon}, spontaneously generated form of PrP carrying the PG14 mutation; PG14^{RML}, Rocky Mountain Laboratory strain of scrapie (RML)-seeded form of PrP carrying the PG14 mutation.
*Chiesa *et al.* 2003
†Moroncini *et al.* 2004; Solforosi *et al.* 2007 and E. Biasini *et al.,* paper submitted.

Table 2 Infectivity of PG14 forms and PrP^{Sc}

	PG14^{Spon}	PG14^{RML}	PrP^{Sc}
Animal transmission	No (Chiesa *et al.* 2003)	Yes (Chiesa *et al.* 2003)	Yes
Seeding activity in PMCA reaction	No	Yes	Yes (Castilla *et al.* 2005)
Co-aggregation with WT PrP or C2 fragment	No	Yes	Yes (Caughey 2001; Chen *et al.* 1995)
Co-aggregation with WT PrP-EGFP	No	NT	Yes (Barmada and Harris 2005)

PG14, nine-octapeptide insertional mutation in prion protein; PrP^{Sc}, scrapie isoform of prion protein; PG14^{Spon}, spontaneously generated form of PrP carrying the PG14 mutation; PG14^{RML}, Rocky Mountain Laboratory strain of scrapie (RML)-seeded form of PrP carrying the PG14 mutation; PMCA, protein misfolding cyclic amplification; WT, wild-type; NT, not tested.

PG14^{RML} particles (Chiesa *et al.* 2003). In this scheme, PG14^{Sol} would be equivalent to the monomeric, α-helical form of PrP, and would represent a common precursor to both PG14^{Spon} and PG14^{RML} aggregates (see cartoon in Table 1). In an alternative scenario, PG14^{Spon} could represent a non-infectious, intermediate state on the pathway that leads from PG14^{Sol} to infectious PG14^{RML}. Intermediate

folding or oligomeric states of recombinant PrP have been described (Apetri *et al.* 2006; Bocharova *et al.* 2006).

To gain further insight into the structural differences between PG14^{Spon} and PG14^{RML}, it will clearly be necessary to purify these forms to homogeneity and to characterize them using spectroscopic, electron microscopic, and chemical modification techniques. Such methods have previously

been applied to oligomeric assemblies generated from recombinant PrP (reviewed in Refs Baskakov and Breydo 2007; Surewicz *et al.* 2006). We anticipate that a similar analysis of PG14^Spon and PG14^RML particles will be particularly fruitful, as these PrP species are derived from brain tissue, and their toxic and infectious properties have been defined *in vivo*.

Implications

Our studies of Tg(PG14) mice suggest that in some prion diseases, toxic, non-infectious forms of PrP such as PG14^Spon, rather than PrP^Sc, may be the proximate cause of neurodegeneration. This conclusion is consistent with a growing body of evidence that the infectivity of prions may be an epi-phenomenon that is not directly related to the mechanisms by which prions induce pathology (Chiesa and Harris 2001; Harris and True 2006). For example, we have suggested that the pathogenicity of PG14^Spon results from gain of a neurotoxic activity that targets synapses, in conjunction with loss of a neuroprotective activity that affects survival of granule neurons (Chiesa *et al.* 2005; Li *et al.* 2007). The identification and characterization of PG14^Spon and other forms of PrP^toxic is important from a therapeutic standpoint, as these species represent attractive drug targets. Indeed, compounds that block propagation of PrP^Sc, without reducing the amount of PrP^toxic or restoring its biological activity, may be ineffective in ameliorating the disease process.

Our results also highlight important similarities between prion diseases and other protein misfolding disorders. A number of human diseases have been found to involve conformational changes in a specific cellular protein, leading to deposition of protein aggregates in brain or other organs with subsequent development of tissue pathology. These disorders, which are not infectious in the conventional sense, include neurodegenerative diseases such as Alzheimer's, Parkinson's, and Huntington's diseases, as well as more than 20 different peripheral amyloidoses (Pepys 2006). PG14^Spon shares key similarities with the protein aggregates found in these other diseases, which are typically characterized by an increase in β-sheet content, alterations in epitope accessibility, and partial resistance to proteolysis. Accumulation of small β-rich oligomers that cause synaptic dysfunction or degeneration may be a common theme in many neurodegenerative disorders because of protein misfolding (Haass and Selkoe 2007).

The results reported here also have implications for the interpretation of analytical tests designed to detect PrP^Sc in clinical or laboratory samples. These tests typically rely upon operational properties such as detergent insolubility, protease resistance, loss or gain of reactivity with PrP-specific antibodies, or NaPTA precipitation to distinguish PrP^Sc from PrP^C (Soto 2004). This study demonstrates that many of the biochemical properties exhibited by PrP^Sc are also found in non-infectious aggregates of PrP. Thus, the development of truly PrP^Sc-specific assays will require additional techniques for selectively recognizing these different PrP species.

Acknowledgements

References

Apetri A. C., Maki K., Roder H. and Surewicz W. K. (2006) Early intermediate in human prion protein folding as evidenced by ultrarapid mixing experiments. *J. Am. Chem. Soc.* **128**, 11673–11678.

Barmada S. J. and Harris D. A. (2005) Visualization of prion infection in transgenic mice expressing green fluorescent protein-tagged prion protein. *J. Neurosci.* **25**, 5824–5832.

Barmada S., Piccardo P., Yamaguchi K., Ghetti B. and Harris D. A. (2004) GFP-tagged prion protein is correctly localized and functionally active in the brains of transgenic mice. *Neurobiol. Dis.* **16**, 527–537.

Baskakov I. V. (2004) Autocatalytic conversion of recombinant prion proteins displays a species barrier. *J. Biol. Chem.* **279**, 7671–7677.

Baskakov I. V. and Breydo L. (2007) Converting the prion protein: what makes the protein infectious. *Biochim. Biophys. Acta* **1772**, 692–703.

Baskakov I. V., Legname G., Baldwin M. A., Prusiner S. B. and Cohen F. E. (2002) Pathway complexity of prion protein assembly into amyloid. *J. Biol. Chem.* **277**, 21140–21148.

Biasini E., Massignan T., Fioriti L., Rossi V., Dossena S., Salmona M., Forloni G., Bonetto V. and Chiesa R. (2006) Analysis of the cerebellar proteome in a transgenic mouse model of inherited prion disease reveals preclinical alteration of calcineurin activity. *Proteomics* **6**, 2823–2834.

Bocharova O. V., Makarava N., Breydo L., Anderson M., Salnikov V. V. and Baskakov I. V. (2006) Annealing prion protein amyloid fibrils at high temperature results in extension of a proteinase K-resistant core. *J. Biol. Chem.* **281**, 2373–2379.

Bolton D. C., Seligman S. J., Bablanian G., Windsor D., Scala L. J., Kim K. S., Chen C. M., Kascsak R. J. and Bendheim P. E. (1991) Molecular location of a species-specific epitope on the hamster scrapie agent protein. *J. Virol.* **65**, 3667–3675.

Brown P., Gibbs C. J., Rodgers-Johnson P., Asher D. M., Sulima M. P., Bacote A., Goldfarb L. G. and Gajdusek D. C. (1994) Human spongiform encephalopathy: the National Institutes of Health series of 300 cases of experimentally transmitted disease. *Ann. Neurol.* **35**, 513–529.

Büeler H., Fischer M., Lang Y., Fluethmann H., Lipp H.-P., DeArmond S. J., Prusiner S. B., Aguet M. and Weissmann C. (1992) Normal development and behavior of mice lacking the neuronal cell-surface PrP protein. *Nature* **356**, 577–582.

Castilla J., Saa P., Hetz C. and Soto C. (2005) In vitro generation of infectious scrapie prions. *Cell* **121**, 195–206.

Caughey B. (2001) Interactions between prion protein isoforms: the kiss of death? *Trends Biochem. Sci.* **26**, 235–242.

Chen S. G., Teplow D. B., Parchi P., Teller J. K., Gambetti P. and Autilio-Gambetti L. (1995) Truncated forms of the human prion protein in normal brain and in prion diseases. *J. Biol. Chem.* **270**, 19173–19180.

Chiesa R. and Harris D. A. (2001) Prion diseases: what is the neurotoxic molecule? *Neurobiol. Dis.* **8**, 743–763.

Chiesa R., Piccardo P., Ghetti B. and Harris D. A. (1998) Neurological illness in transgenic mice expressing a prion protein with an insertional mutation. *Neuron* **21**, 1339–1351.

Chiesa R., Drisaldi B., Quaglio E., Migheli A., Piccardo P., Ghetti B. and Harris D. A. (2000) Accumulation of protease-resistant prion protein (PrP) and apoptosis of cerebellar granule cells in transgenic mice expressing a PrP insertional mutation. *Proc. Natl Acad. Sci. USA* **97**, 5574–5579.

Chiesa R., Piccardo P., Quaglio E., Drisaldi B., Si-Hoe S. L., Takao M., Ghetti B. and Harris D. A. (2003) Molecular distinction between pathogenic and infectious properties of the prion protein. *J. Virol.* **77**, 7611–7622.

Chiesa R., Piccardo P., Dossena S., Nowoslawski L., Roth K. A., Ghetti B. and Harris D. A. (2005) *Bax* deletion prevents neuronal loss but not neurological symptoms in a transgenic model of inherited prion disease. *Proc. Natl Acad. Sci. USA* **102**, 238–243.

Deleault N. R., Geoghegan J. C., Nishina K., Kascsak R., Williamson R. A. and Supattapone S. (2005) Protease-resistant prion protein amplification reconstituted with partially purified substrates and synthetic polyanions. *J. Biol. Chem.* **280**, 26873–26879.

Duchen L. W., Poulter M. and Harding A. E. (1993) Dementia associated with a 216 base pair insertion in the prion protein gene: clinical and neuropathological features. *Brain* **116**, 555–567.

Haass C. and Selkoe D. J. (2007) Soluble protein oligomers in neurodegeneration: lessons from the Alzheimer's amyloid beta-peptide. *Nat. Rev. Mol. Cell. Biol.* **8**, 101–112.

Harris D. A. and True H. L. (2006) New insights into prion structure and toxicity. *Neuron* **50**, 353–357.

Kong Q., Surewicz W. K., Petersen R. B. *et al.* (2004) Inherited prion diseases, in *Prion Biology and Diseases* (Prusiner S. B., ed.), pp. 673–775. Cold Spring Harbor Laboratory Press, Cold Spring Harbor, NY.

Korth C., Stierli B., Streit P. *et al.* (1997) Prion (PrP^{Sc})-specific epitope defined by a monoclonal antibody. *Nature* **390**, 74–77.

Kramer M. L., Kratzin H. D., Schmidt B., Romer A., Windl O., Liemann S., Hornemann S. and Kretzschmar H. (2001) Prion protein binds copper within the physiological concentration range. *J. Biol. Chem.* **276**, 16711–16719.

Krasemann S., Zerr I., Weber T., Poser S., Kretzschmar H., Hunsmann G. and Bodemer W. (1995) Prion disease associated with a novel nine octapeptide repeat insertion in the PRNP gene. *Mol. Brain Res.* **34**, 173–176.

Lee I. S., Long J. R., Prusiner S. B. and Safar J. G. (2005) Selective precipitation of prions by polyoxometalate complexes. *J. Am. Chem. Soc.* **127**, 13802–13803.

Legname G., Baskakov I. V., Nguyen H. O., Riesner D., Cohen F. E., DeArmond S. J. and Prusiner S. B. (2004) Synthetic mammalian prions. *Science* **305**, 673–676.

Legname G., Nguyen H. O., Peretz D., Cohen F. E., DeArmond S. J. and Prusiner S. B. (2006) Continuum of prion protein structures enciphers a multitude of prion isolate-specified phenotypes. *Proc. Natl Acad. Sci. USA* **103**, 19105–19110.

Li A., Piccardo P., Barmada S. J., Ghetti B. and Harris D. A. (2007) Prion protein with an octapeptide insertion has impaired neuroprotective activity in transgenic mice. *EMBO J.* **26**, 2777–2785.

Miller T. M. and Johnson E. M. Jr (1996) Metabolic and genetic analyses of apoptosis in potassium/serum-deprived rat cerebellar granule cells. *J. Neurosci.* **16**, 7487–7495.

Millhauser G. L. (2007) Copper and the prion protein: methods, structures, function, and disease. *Annu. Rev. Phys. Chem.* **58**, 299–320.

Moroncini G., Kanu N., Solforosi L. *et al.* (2004) Motif-grafted antibodies containing the replicative interface of cellular PrP are specific for PrP^{Sc}. *Proc. Natl Acad. Sci. USA* **101**, 10404–10409.

Nazor K. E., Kuhn F., Seward T. *et al.* (2005) Immunodetection of disease-associated mutant PrP, which accelerates disease in GSS transgenic mice. *EMBO J.* **24**, 2472–2480.

Novitskaya V., Bocharova O. V., Bronstein I. and Baskakov I. V. (2006) Amyloid fibrils of mammalian prion protein are highly toxic to cultured cells and primary neurons. *J. Biol. Chem.* **281**, 13828–13836.

Owen F., Poulter M., Collinge J., Leach M., Lofthouse R., Crow T. J. and Harding A. E. (1992) A dementing illness associated with a novel insertion in the prion protein gene. *Mol. Brain Res.* **13**, 155–157.

Pan T., Li R., Kang S. C., Wong B. S., Wisniewski T. and Sy M. S. (2004) Epitope scanning reveals gain and loss of strain specific antibody binding epitopes associated with the conversion of normal cellular prion to scrapie prion. *J. Neurochem.* **90**, 1205–1217.

Pastrana M. A., Sajnani G., Onisko B., Castilla J., Morales R., Soto C. and Requena J. R. (2006) Isolation and characterization of a proteinase K-sensitive PrP^{Sc} fraction. *Biochemistry* **45**, 15710–15717.

Pepys M. B.(2006) Amyloidosis. *Annu. Rev. Med.* **57**, 223–241.

Piccardo P., Manson J. C., King D., Ghetti B. and Barron R. M. (2007) Accumulation of prion protein in the brain that is not associated with transmissible disease. *Proc. Natl Acad. Sci. USA* **104**, 4712–4717.

Prusiner S. B.(1998) Prions. *Proc. Natl Acad. Sci. USA* **95**, 13363–13383.

Saa P., Castilla J. and Soto C. (2006) Ultra-efficient replication of infectious prions by automated protein misfolding cyclic amplification. *J. Biol. Chem.* **281**, 35245–35252.

Saborio G. P., Permanne B. and Soto C. (2001) Sensitive detection of pathological prion protein by cyclic amplification of protein misfolding. *Nature* **411**, 810–813.

Safar J., Wille H., Itrri V., Groth D., Serban H., Torchia M., Cohen F. E. and Prusiner S. B. (1998) Eight prion strains have PrP^{Sc} molecules with different conformations. *Nature Med.* **4**, 1157–1165.

Shaked Y., Rosenmann H., Hijazi N., Halimi M. and Gabizon R. (2001) Copper binding to the prp isoforms: a putative marker of their conformation and function. *J. Virol.* **75**, 7872–7874.

Silveira J. R., Raymond G. J., Hughson A. G., Race R. E., Sim V. L., Hayes S. F. and Caughey B. (2005) The most infectious prion protein particles. *Nature* **437**, 257–261.

Solforosi L., Bellon A., Schaller M., Cruite J. T., Abalos G. C. and Williamson R. A. (2007) Toward molecular dissection of PrP^{C}–PrP^{Sc} interactions. *J. Biol. Chem.* **282**, 7465–7471.

Soto C. (2004) Diagnosing prion diseases: needs, challenges and hopes. *Nat. Rev. Microbiol.* **2**, 809–819.

Stöckel J., Safar J., Wallace A. C., Cohen F. E. and Prusiner S. B. (1998) Prion protein selectively binds copper(II) ions. *Biochemistry* **37**, 7185–7193.

Surewicz W. K., Jones E. M. and Apetri A. C. (2006) The emerging principles of mammalian prion propagation and transmissibility barriers: insight from studies in vitro. *Acc. Chem. Res.* **39**, 654–662.

Swietnicki W., Morillas M., Chen S. G., Gambetti P. and Surewicz W. K. (2000) Aggregation and fibrillization of the recombinant human prion protein huPrP90–231. *Biochemistry* **39**, 424–431.

Tanaka M., Collins S. R., Toyama B. H. and Weissman J. S. (2006) The physical basis of how prion conformations determine strain phenotypes. *Nature* **442**, 585–589.

Tateishi J. and Kitamoto T. (1995) Inherited prion diseases and transmission to rodents. *Brain Pathol.* **5**, 53–59.

Tzaban S., Friedlander G., Schonberger O., Horonchik L., Yedidia Y., Shaked G., Gabizon R. and Taraboulos A. (2002) Protease-sensitive

scrapie prion protein in aggregates of heterogeneous sizes. *Biochemistry* **41**, 12868–12875.

Wadsworth J. D., Joiner S., Hill A. F., Campbell T. A., Desbruslais M., Luthert P. J. and Collinge J. (2001) Tissue distribution of protease resistant prion protein in variant Creutzfeldt-Jakob disease using a highly sensitive immunoblotting assay. *Lancet* **358**, 171–180.

Weissmann C. (2004) The state of the prion. *Nat. Rev. Microbiol.* **2**, 861–871.

Westergard L., Christensen H. M. and Harris D. A. (2007) The cellular prion protein (PrP^C): its physiological function and role in disease. *Biochim. Biophys. Acta* **1772**, 629–644.

Yuan J., Xiao X., McGeehan J. *et al.* (2006) Insoluble aggregates and protease-resistant conformers of prion protein in uninfected human brains. *J. Biol. Chem.* **281**, 34848–34858.

Zanusso G., Liu D., Ferrari S. *et al.* (1998) Prion protein expression in different species: analysis with a panel of new mAbs. *Proc. Natl Acad. Sci. USA* **95**, 8812–8816.